

Interconnection Networks for Scalable Quantum Computers

Nemanja Isailovic, Yatish Patel, Mark Whitney, John Kubiatowicz
Computer Science Division
University of California, Berkeley
{nemanja, yatish, whitney, kubitron}@cs.berkeley.edu

Abstract

We show that the problem of communication in a quantum computer reduces to constructing reliable quantum channels by distributing high-fidelity EPR pairs. We develop analytical models of the latency, bandwidth, error rate and resource utilization of such channels, and show that 100s of qubits must be distributed to accommodate a single data communication. Next, we show that a grid of teleportation nodes forms a good substrate on which to distribute EPR pairs. We also explore the control requirements for such a network. Finally, we propose a specific routing architecture and simulate the communication patterns of the Quantum Fourier Transform to demonstrate the impact of resource contention.

1. Introduction

Quantum computing utilizes properties of subatomic physics to compute in ways unavailable to classical computers. As interesting as they may be to contemplate, quantum computers face a number of barriers to their implementation, such as the fragility of quantum information and the lack of systematic techniques for moving such information within the fabric of a quantum computer. This paper seeks to address the latter problem.

It would appear that quantum computers must reach a capacity to process and store a few thousand quantum bits (or “qubits”) before becoming competitive with classical machines. Since the information contained within a qubit is extremely fragile, the qubits utilized by algorithms (called “logical qubits”) are often implemented by encoding 10s or 100s of physical components (“physical qubits”) using Error Correction Codes (ECC). Combine this fact with the need for many temporary qubits (called “ancillae”) in quantum algorithms, and we can conclude that an effective quantum datapath can easily contain a million physical qubits. We will use “qubit” to refer to a physical qubit and “logical qubit” explicitly to refer to an encoded state of many qubits.

Anytime such a large number of bits must interact, communication issues arise: how exactly should we schedule and route information? Several observations narrow the space of answers to this question. First, in all technologies currently under study, two qubits must be physically adjacent in order to compute a two-input function on these qubits. This means that all of the physical qubits comprising

one logical qubit must be moved adjacent to those comprising a second logical qubit when computing; as a result, each two-input computation entails movement of 10s or 100s of qubits. Second, it is not uncommon for quantum algorithms to require all-to-all communication during some portion of their execution. For example, the Quantum Fourier Transform (QFT) [21], a component of Shor’s factorization algorithm [25], requires all-to-all communication. Third, the routing of qubits must be timed to coincide with the arrival of opcodes to various functional units.

While a million bits of storage is not particularly large by classical silicon standards, it *is* large when taking into account the degradation of state experienced by a qubit through movement. As discussed in Section 4, for instance, a qubit in an Ion-Trap computer experiences a probability of corruption of about 10^{-6} when physically transported the distance of a single storage bit at maximum density. Structuring a million qubits as a dense 1000×1000 grid, this means that a qubit would experience a probability of error of more than 10^{-3} in traveling from corner to corner. Clearly, this is an unacceptable level of error, leading us to consider other options for moving information.

One solution is to use teleportation [22] in which data is moved indirectly: after high-fidelity, entangled helper qubits (called *EPR pairs*) are sent to the endpoints of the desired communication, they are utilized to transfer the state of a logical qubit using local quantum operations and reliable classical communication. Although EPR pairs experience the same degradation during movement as data qubits, they represent known states; consequently multiple lower-fidelity EPR pairs can be combined at the endpoints to produce high-fidelity EPR pairs through a process called *purification*. The process of distributing high-fidelity EPR pairs to communication endpoints can be viewed as setting up a reliable “quantum channel” and is our primary topic.

In the following, we explore architectures for constructing reliable quantum channels in a large quantum computer. We start with some background in Section 2. In Section 3, we discuss architectural options for distributing EPR pairs and constructing quantum channels. We show that routing of EPR pairs to either end of arbitrary points on a quantum computer exhibits much similarity to routing in classical multiprocessor networks. Next, in Section 4, we explore the physical resources required to produce high-fidelity EPR pairs. One problem that we illuminate is that the archi-

texture of the network can greatly influence the number of raw EPR pairs required to set up a communication channel. We continue in Section 5 with a simulation of kernels from Shor’s factorization algorithm on a machine that utilizes dimension-ordered mesh routing to distribute EPR pairs. Finally, we conclude in Section 6.

2. Overview

In this section, we present an overview of the important aspects of a quantum computer. For concreteness in our analysis, we shall assume the use of ion trap technology [14], which has been studied and demonstrated on a small scale in various experiments [17].

2.1. High-level viewpoint

As shown in Figure 1, our view of a quantum computer revolves around its quantum datapath. A set of functional units is connected through a flexible routing infrastructure. A classical control unit transforms a stream of instructions (the quantum algorithm) into control for both the functional units and the routing infrastructure.

This figure shows each functional unit operating on one or two logical qubits. Functional units must contain registers large enough to hold their input arguments. Further, we assume that at least one (and possibly both) of these registers is capable of holding a logical qubit for an extended period of time (i.e. capable of continuous error correction). Although functional units would appear to contain very little logic, they are in fact rather large, due to the number of physical qubits that comprise a single logical qubit¹.

We envision routing to be a two-level process. The classical control unit schedules communication by specifying a series of logical qubit movements and functional unit operations. Classical control logic within the interconnection network is responsible for efficiently (and reliably) moving physical qubits as requested by the classical control.

This architecture is justified in the following manner: First, the number of logical qubits in the system is (relatively) small, leading to a tractable pairwise scheduling problem for the top-level scheduler. Second, the number of physical qubits that must be moved in response to a high level communication request is quite large (especially when considering raw EPR pairs, as discussed in Section 4). Once a path is constructed from source to destination, the process of moving these qubits requires relatively simple (but frequent) control. Finally, the size of a functional unit coupled with the need for flexible point-to-point communication leads us to consider structured routing networks. An analogy with multiprocessor networking is very appropriate here, with functional units similar to compute nodes.

¹Note that more complex functional units are certainly possible, but they are outside the scope of this paper.

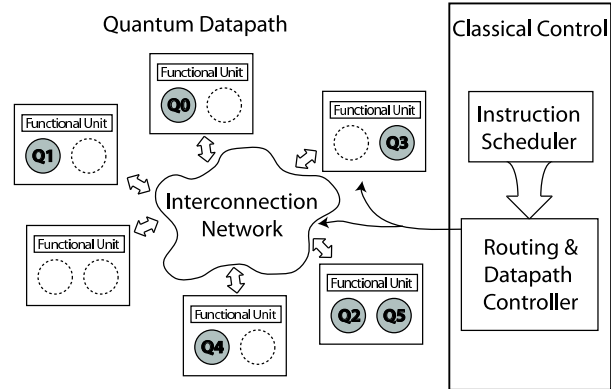


Figure 1: Abstract view of the quantum datapath. Each functional unit contains space for two logical qubits, which may be used for interaction or storage. A classical instruction scheduler and datapath control unit initiate communication and computation.

2.2. Qubits

A quantum bit (qubit) is a bit of information encoded in a two-level quantum system. The underlying physics of such two-level systems is potentially quite complicated, but for the purposes of this paper, we will present a simplified view. In an ion trap quantum computer, each qubit is a single ion. A qubit has some state, which is analogous to a classical bit’s value of 0 or 1, although it can include a *superposition* or mixture of the two values. Computation consists of one-qubit and/or two-qubit gates within functional units [14].

Qubit state is quite fragile. Current experimental results show the error rate of a single quantum gate to be around 10^{-3} [17]. Advances in the near future could reduce this number down to $10^{-6} - 10^{-8}$ [19, 29], but it is pretty clear that it will be a long time (if ever) before we reach error rates found in traditional CMOS gates (10^{-19}) [8]. Even worse, errors can occur during simple qubit movement, with error probability growing with distance. These shortcomings have prompted the development of *quantum* error correcting codes [16, 26, 27] for quantum data. Quantum ECC codes, much like classical codes, encode a single bit of data into multiple real bits (ions).

The use of quantum ECC codes leads us to the important distinction between physical and logical qubits. A physical qubit is a single positively charged ion, while a logical qubit is specified as a bit of data used in the computation. Physically, a logical qubit is encoded in some number of physical qubits. As mentioned previously, we will use the term “qubit” to refer to a physical qubit, while “logical qubit” will be stated explicitly. Logical qubits must be corrected continuously, before, during and after computation or movement, in order to combat the ever-present tendency to decohere. It is not uncommon to see proposals to use 49 or 343 physical qubits to encode one logical qubit.

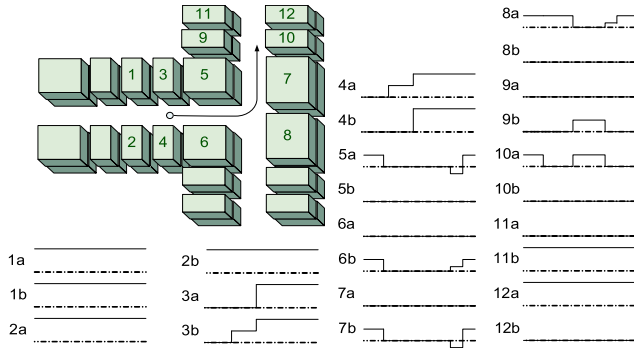


Figure 2: Electrode layout and waveforms to move a physical qubit (positively charged ion) from between electrodes 3 and 4 to between 9 and 10. Gray solids are electrodes; white space between them is the channel. The dashed line in each waveform is ground; a and b refer to top and bottom electrodes at each location.

2.3. Communication

Quantum operations involving two logical qubits require the logical qubits to be physically adjacent. One of the biggest restrictions to qubit movement is the *no-cloning theorem* [30] that states that it is impossible to make a copy of a qubit that is in an arbitrary state. Consequently, there is no fan-out in a quantum datapath, and quantum state must be actively moved to an interaction site before it can participate in a computation. Thus, qubits stored in non-adjacent parts of our datapath must undergo a significant amount of movement to perform a two-qubit gate. In the following, we discuss two techniques to transfer the state of a qubit from one point to another.

Ballistic Transport: An ion trap consists of a set of electrodes which trap an ion in the space between them. By placing several ion traps in sequence and applying specific pulse sequences to the electrodes, we can ballistically transport the ion along the channel, thus yielding a simple wire.

Figure 2 shows a simplified view of a few ion traps [9], as well as control pulses required to move an ion through these traps. There have been demonstrations of MEMS fabrication techniques that could scale to produce many integrated qubits [18]. In this figure, the gray solids are electrodes. The white space between them is the ballistic channel. Ballistic transport is the most basic communication operation in an ion-trap computer. As illustrated by Figure 2, this seemingly simple operation is relatively complex.

Ballistic movement of a qubit causes some loss in the fidelity of its state (called decoherence). Thus, there is a limit to the distance that a qubit may be moved ballistically before error correction must be performed [11]. There is general consensus that any reasonably sized chip will require an additional form of communication for longer distances.

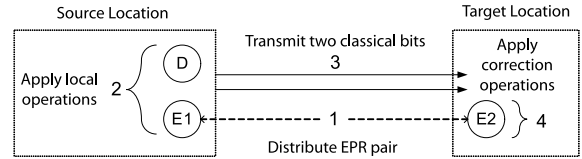


Figure 3: Teleporting data qubit D to the target location requires (1) a high-fidelity EPR pair (E1/E2), (2) local operations at the source, (3) transmission of classical bits, and (4) correction operations to recreate D from E2 at the target.

Teleportation: Figure 3 gives an abstract view of teleportation [3]. We wish to transmit the state of physical data qubit D from the source location to some distant target location without physically moving the data qubit (since that would result in too much decoherence).

We start by interacting a pair of qubits (E1 and E2) to produce a joint quantum state called an *EPR pair*. Qubits E1 and E2 are generated together and then sent to either endpoint. Next, local operations are performed at the source location, resulting in two classical bits and the destruction of the state of qubits D and E1. Through quantum entanglement, qubit E2 ends up in one of four transformations of qubit D’s original state. Once the two classical bits are transmitted to the destination, local correction operations can transform E2 into an exact replica of qubit D’s original state². The only non-local operations in teleportation are the transport of an EPR pair to source and destination and the later transmission of classical bits from source to destination (which requires a classical communication network).

We can view the delivery of the EPR pair as the process of *constructing a quantum channel* between source and destination. This EPR pair must be of high fidelity to perform reliable communication. As discussed in Section 4, purification permits a tradeoff between channel setup time and fidelity. Since EPR pair distribution can be performed in advance, qubit communication time can approach the latency of classical communication; of course, channel setup time grows with distance as well as fidelity.

3. Communication Infrastructure

A quantum program execution consists of a sequence of one- and two-qubit gates applied to a finite set of logical qubits. The program is run by applying these gates as quickly as possible, stalling as necessary at each functional unit to wait for logical qubit operands. A classical scheduler determines which logical communications occur and when. Error correction of logical qubits and fault tolerant gate implementation are handled at the scheduler level.

As explained in Section 2, ballistic movement of logical

²Notice that the no-cloning theorem is not violated since the state of qubit D is destroyed in the process of creating E2’s state.

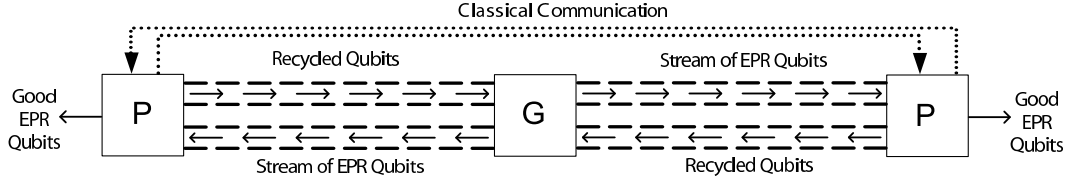


Figure 4: Ballistic Movement Distribution Methodology: EPR pairs are generated in the middle and ballistically moved using electrodes. After purification, high-fidelity EPR qubits are moved to the logical qubits, used, and then recycled into new EPR pairs.

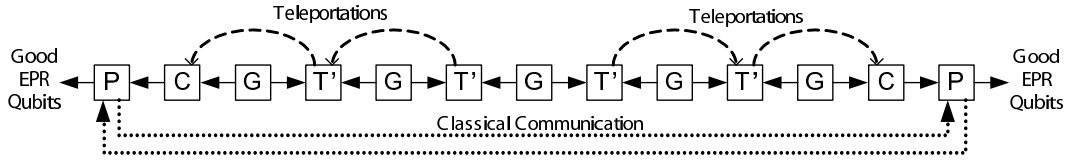


Figure 5: Chained Teleportation Distribution Methodology: EPR qubits generated at the midpoint generator are successively teleported until they reach the endpoint teleporter nodes before being ballistically moved to corrector nodes and then purifier nodes.

qubits results in far too much decoherence to be practical. Thus, the problem of arranging for logical communication comes down to distributing EPR pairs to the endpoints to allow teleportation of the logical qubit.

3.1. Distribution Methodology

One option for EPR pair distribution is to generate EPR pairs at generator (G) nodes in the middle of the path and ballistically transport them to purifier (P) nodes that are close to the endpoints, as shown in Figure 4. Purification combines two EPR pairs to produce a single one of higher fidelity. For each qubit in the left purification (P) node, its entangled partner is in the right P node undergoing the same operations. For each purification performed, one classical bit is sent from each end to the opposite one. Discarded qubits are returned to the generator for reuse.

Another option is to generate an EPR pair and perform a sequence of teleportation operations to transmit these pairs to their destination. Correction information from a teleportation (two classical bits) can be accumulated over multiple teleportations and performed in aggregate at each end of the chain. This process is depicted in Figure 5. A T' node contains units that perform the local operations to entangle qubits (step 2 in Figure 3), but no correction capability (step 4 in Figure 3). Instead, each T' node updates correction information and passes it to the next hop in the chain.

The path consists of alternating G nodes and T' nodes, with a C node and a P node at each end. Each G node sends EPR pairs to adjacent T' nodes. The EPR pairs generated at the central G node are moved ballistically to the nearest T' nodes, then successively teleported from T' node to T' node using the EPR pairs generated by the other G nodes. Since the EPR pairs along the length of the path can be pre-distributed, this method can improve the latency of the distribution if the T' nodes are spaced far enough apart.

Between each pair of “adjacent” T' nodes (as defined by network topology) is a G node continually generating EPR pairs and sending one qubit of each pair to each adjacent T' node. Thus, each T' node is constantly linked with each neighboring T' node by these incoming streams of entangled EPR qubits. Each G node is essentially creating a *virtual wire* which connects its endpoint T' nodes, allowing teleportation between them.

To permit general computation, any functional unit must have a nearby T' node (although they may be shared). This implies the necessity of a grid of T' nodes across the chip, which are linked as described above by virtual wires. The exact topology is an implementation choice; one need not link physically adjacent or even nearby T' nodes, so long as enough channels are included to allow each G node to be continuously linking the endpoint T' nodes of its virtual wire with a steady stream of EPR qubits. Thus, any routing network could be implemented on this base grid of T' nodes, such as a butterfly network or a mesh grid.

3.2. Structuring Global Communication

As we discussed in Section 2.3, the process of moving quantum bits ballistically from point to point presents a challenging control problem. Designing control logic to move ions along a well-defined path appears tractable. However, controlling every electrode to select one of many possible paths becomes much more complex. Thus, we can benefit from restricting the paths that ions can take within our quantum computer. Such a tractable control structure will involve a sequence of “single-path” channels (much like wires in a classical architecture) connecting router-like control points.

We assume a mesh grid of routers as a reasonable first-cut at a general purpose routing network [1, 5]. Under the Ballistic Movement Distribution Methodology (Figure 4), a

routing channel is a straight sequence of ion traps, while a router is at the intersection. Under the Chained Teleportation Distribution Methodology (Figure 5), a router is a T' node, and a routing channel is the pre-generated link between two T' nodes. In either case, there must be G nodes distributed across the chip to generate EPR pairs.

Route Planning: High-level classical control views the quantum datapath at the logical level. It tracks the current location of each logical qubit but knows nothing of the actual encoding used (*i.e.* number of physical qubits per logical qubit). This control takes the sequence of logical operations that comprise the program and identifies all logical communications that need to occur. It then begins routing them while maintaining program order.

Once a path has been determined, EPR pairs need to be generated and routed to the endpoints for purification. A G node near the middle of the path is given instructions by the high-level control to generate and name EPR pairs. These EPR qubits are then sent from router to router (whether intersection or T' node) along the routing channels (whether ion traps or teleportation links) until the endpoints are reached, at which point they are locally routed to the purifiers. Thus, under either methodology, the routers need only be able to make local routing decisions based on a qubit's destination.

Local Routing Control: Each router and G node needs local classical control to determine how it handles qubits, which requires a means of identifying qubits. Thus, each qubit is associated with a classical message which travels alongside the qubit in a parallel classical network. The node control for the G node which generates a pair also generates their accompanying messages. A qubit's message contains the ID assigned by the G node, the destination of this qubit, the destination of its partner (which is necessary for the purification steps at the endpoints), and space for the cumulative correction information that will be used at the endpoint. A router forwards a qubit on to the appropriate routing channel or to a local corrector at the destination.

Figure 6 shows one possible implementation for a router. The router receives a constant stream of EPR pairs (from G nodes) linking it to its neighbor routers. During an incoming teleportation, a qubit enters the Storage area to wait for the operations at the teleportation source to complete. Classical data in the form of the teleporting qubit's ID packet and the two classical bits used in the teleportation enter the adjoining classical control (CC). The cumulative correction information is updated in the ID packet, and the destination information is used to route the qubit to the correct set of teleporters (or to the nearby C node if this is the endpoint). For an outgoing teleportation, a qubit from the G node stream bypasses the Storage area and moves directly

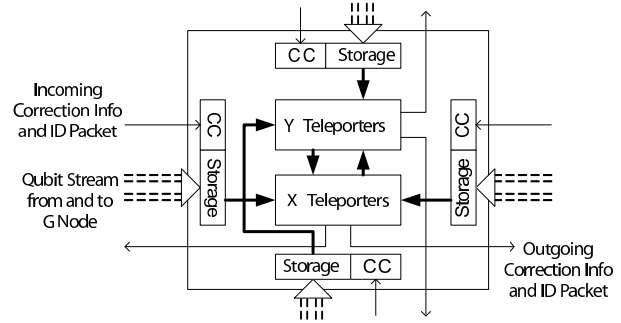


Figure 6: A Quantum Router: Two sets of teleporters implement dimension-order routing. Fat arrows are incoming qubits from a G node (and recycled ions in opposite direction). Bold arrows are ion movement within router. Thin arrows are classical data. CC is the classical control including cumulative correction information and further routing.

to the appropriate teleporter.

In this router design, the teleporters are divided into two sets. One set handles all traffic moving in the X direction, the other handles traffic moving in the Y direction. For a turn, an EPR qubit must be ballistically moved between the teleporter sets (as shown by the bold-headed arrows). It is evident from the crossing arrows in the figure that streams of qubits may need to cross. However, even with stalling, movement time is so much faster than teleportation (Table 1) that crossing will not be a limiting factor.

3.3. Metrics

We shall evaluate various approaches to the EPR distribution mechanism using six metrics.

Error Rate: Ballistic transport and teleportation both cause qubits to decohere. The architectural design must take into account the number of operations each qubit will undergo and the resulting chance for errors.

EPR Pair Count: While most operations cause qubits to decohere, purification actually decreases error chance on one pair by sacrificing one or more other pairs. The more error that is accumulated, the more pairs will need to be transported to the endpoints.

Latency: Logical communication set-up time determines how far in advance EPR distribution must occur.

Quantum Resource Needs: The quantum datapath resource needs (quantity of each component) affect chip area and thus communication distance.

Classical Control Complexity: Generation, ballistic movement, teleportation and purification must each be controlled classically, so the classical control requirements vary with communication methodology.

Runtime: Ultimately, we want to know the impact of long distance communication setup on execution time.

4. Qubit Communication Models

In this section, we analyze the communication channels introduced in the last section. Before we do this, however, we need to introduce an important measure called *fidelity* for measuring the difference between two quantum states.

4.1. Fidelity

Fidelity measures the difference between two quantum bit vectors. Because of quantum entanglement, each of the 2^n combinations of bits in a vector of size n are physically separate states. For a given problem, one particular vector is considered a reference state that other vectors are compared against. For example, if we start with a bit vector of zeros [0000], and we send the bits through a noisy channel in which bit 3 is flipped with probability p , we would end up with a probabilistic vector of $((1-p)[0000] + p[0010])$. The fidelity of the final state in relation to the starting (“error-free”) state is just $1 - p$. So, in the case of an operational state vs. a reference “correct” state, the fidelity describes the amount of error introduced by the system on the operational state [21]. A fidelity of 1 indicates that the system is definitely in the reference state. A fidelity of 0 indicates that the system has no overlap with the reference state.

We characterize errors by calculating the fidelity of qubits traversing the various quantum channels and gates necessary to route and move bits around a communication network. We will combine models of the individual communication components so that we get an overall *fidelity of communication* as a function of distance and architecture.

4.2. Ion Trap Parameters

For the remainder of the paper, we utilize parameters for ion trap quantum computers. We use the experimental values for time constants shown in Table 1 [19, 23, 24]. A “cell” refers to the minimum distance of a ballistic move (one ion trap). Both teleportation and purification require classical bits to be routed between the endpoints, and thus both of these numbers vary with distance. Further, every quantum operation other than purification results in errors (loss of fidelity). Table 2 lists the error probabilities used for the following fidelity calculations.

4.3. Ballistic Transport Model

In ballistic movement, the fidelity of a bit after going through the ballistic channel over D cells is:

$$F_{new} = F_{old}(1 - p_{mv})^D \quad (1)$$

since each hop introduces a probability of error. The time to perform ballistic movement is given in time per cell moved through and from Table 1 is $0.2\mu s/cell$.

$$t_{ballistic} = t_{mv} \times D \quad (2)$$

Operation	Variable Name	Time (μs)
One-Qubit Gate	t_{1q}	1
Two-Qubit Gate	t_{2q}	20
Move One Cell	t_{mv}	0.2
Measure	t_{ms}	100
Generate	t_{gen}	122
Teleport	t_{prt}	~ 122
Purify	t_{prfy}	~ 121

Table 1: Time constants for operations in ion trap technology. One cell is the minimum distance for ballistic movement (one ion trap).

Operation	Variable Name	Error Probability
One-Qubit Gate	p_{1q}	10^{-8}
Two-Qubit Gate	p_{2q}	10^{-7}
Move One Cell	p_{mv}	10^{-6}
Measure	p_{ms}	10^{-8}

Table 2: Error probability constants for various operations in ion trap technology. Estimates come from [19, 29].

4.4. Teleportation Transport Model

The fidelity of a qubit teleportation is more complicated because it involves a combination of single and double qubit gates (p_{1q}, p_{2q}) and qubit measurement (p_{ms}) [7]:

$$F_{new} = \frac{1}{4} \left(1 + 3(1 - p_{1q})(1 - p_{2q}) \frac{(4(1 - p_{ms})^2 - 1)}{3} \right) \times \frac{(4F_{old} - 1)(4F_{EPR} - 1)}{9} \quad (3)$$

The fidelity after a teleportation involves the fidelity of the data before teleportation (F_{old}) and the fidelity of the EPR pair used to perform the teleportation (F_{EPR}).

Although ballistic movement error does not appear in this formula, it should be mentioned that the fidelity of the EPR pair will be degraded while being distributed to the endpoints of the teleportation channel. Thus, even though the qubit undergoing teleportation incurs no error from direct ballistic movement, there is still fidelity degradation due to EPR pair distribution.

We produce EPR pairs from two qubits initialized to the zero state using a few single and double qubit gates. The fidelity of an EPR pair immediately after generation is:

$$F_{gen} \propto (1 - p_{1q})(1 - p_{2q})F_{zero} \quad (4)$$

F_{zero} is the fidelity of the starting zeroed qubits. Generation time involves one single and one double qubit gate. As mentioned in Table 1, this time is projected to be $21\mu s$.

If we assume that EPR pairs are already located at the endpoints of our channel, teleportation time is given in Ta-

ble 1 as $122\mu s$ and has the form:

$$t_{teleport} = 2t_{1q} + t_{2q} + t_{ms} + t_{classical\ bit\ mv} \times D \quad (5)$$

4.5. EPR Purification Model

As shown by Equation 3, the fidelity of the EPR pairs utilized in teleportation (F_{EPR}) has a direct impact on the fidelity of information transmitted through the teleportation channel. Since EPR pairs accrue errors during ballistic movement, teleportation by itself is not an improvement over direct ballistic movement of data qubits unless some method can be utilized to improve the fidelity of EPR pairs.

Purification combines two lower-fidelity EPR pairs with local operations at either endpoint to produce one pair of higher fidelity; the remaining pair is discarded after being measured. Figure 7 illustrates this process, which must be synchronized between the two endpoints since classical information is exchanged between them. On occasion both qubits will be discarded (with low probability).

The purification process can be repeated in a tree structure to obtain higher fidelity EPR pairs. Each *round* of purification corresponds to a level of the tree in which all EPR pairs have the same fidelity. Since one round consumes slightly more than half of the remaining pairs, resource usage is exponential in the number of rounds. There are two similar tree purification protocols, the DEJMPS protocol [6] and the BBPSSW protocol [2]. The analysis of the DEJMPS protocol provides tighter bounds which assures faster, higher fidelity-producing operation compared to the BBPSSW protocol. The effects are significant, implying that purification mechanisms must be considered carefully³.

Figure 8 shows error rate as a function of number of purification rounds. The BBPSSW protocol takes 5-10 times more rounds to converge to its maximum value as the DEJMPS protocol. Since EPR pair consumption is exponential in number of rounds, the purification protocol has a large impact on total EPR resources needed for communication. Other features of Figure 8 to note are that DEJMPS has higher maximum fidelity and converges to maximum fidelity faster than BBPSSW (possibly because BBPSSW partially randomizes its state after every round).

Finally, the time to purify a set of EPR qubits is dependent on the initial and desired fidelity. The time to complete one round of purification is $121\mu s$ from Table 1:

$$t_{purify\ round} = t_{2q} + t_{ms} + t_{classical\ bit} \quad (6)$$

4.6. Communication Model Analysis

We know from the most recent version of the threshold theorem for fault-tolerant quantum computation that data qubit fidelity must be maintained above $1 - 7.5 * 10^{-5}$ [28].

³Dur also proposes a linear approach to purification [7]; unfortunately, it appears to be sensitive to the error profile. We will not analyze it here.

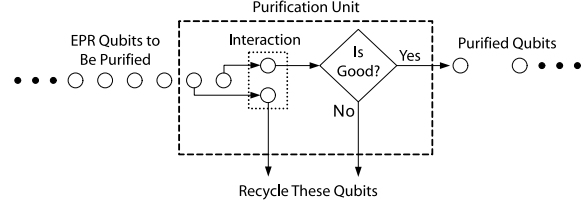


Figure 7: Simple Purification: pairs of EPR qubits undergo local operations, yielding a classical bit that is exchanged with the partner unit. Purification succeeds if classical bits are equal.

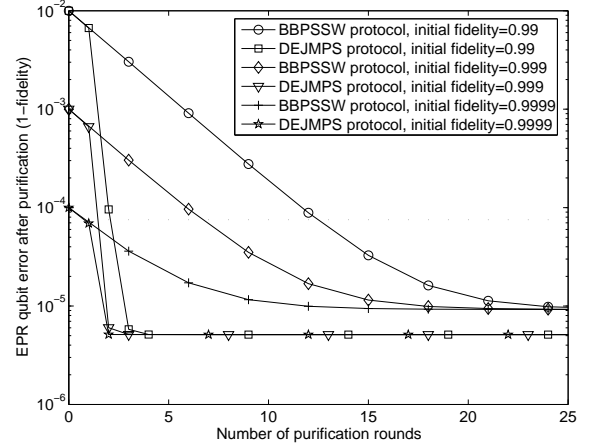


Figure 8: Error rate (1-fidelity) for surviving EPR pairs as a function of the number of purification rounds (tree levels) performed by the DEJMPS or BBPSSW protocol. Lower is better.

Because the preservation of data qubit fidelity is our highest priority, we choose to transport all data by way of single teleports, since this introduces the minimum error from ballistic movement. Additionally, to minimize the number of interactions with expendable, lower fidelity EPR pairs, we choose to move a data qubit with a single, long-distance teleportation. This necessitates the distribution of EPR pair qubits to communication endpoints. Since data qubits interact with these EPR pairs, the above threshold must be imposed on them to avoid tainting the data.

Two options present themselves for distributing high-quality EPR pairs to channel endpoints. First, one could ballistically move the EPR pairs to the endpoints, which is preferable to moving data ballistically because EPR pairs can be sacrificed if they accumulate too much error. Second, one could route EPR pairs through a series of teleporters, as shown in Figure 5. While preserving fidelity of our data states is top priority, when dealing with less precious EPR pairs, we do not have to adhere to strict maximal fidelity preserving distribution methods. In the rest of this section, we will investigate the tradeoffs between ballistic distribution and chained teleportation distribution of EPR pairs.

Fidelity Difference: The final fidelity of these two tech-

niques is approximately the same. Conceptually, the final EPR pair either directly accumulates movement error (through ballistic movement) or is interacted with several other EPR pairs to teleport it to the endpoints and these intermediate EPR pairs have accumulated the same distance ballistically. By interacting with intermediate pairs, the final pair accumulates all this error. This statement assumes that the fidelity loss from gate error is much less than the loss due to ballistic movement, which is the case for ion traps, as shown in Table 1 (for two teleporters spaced 100 cells apart, ballistic movement error equals $1 - (1 - 10^{-6})^{100} \approx 10^{-4}$ compared to 10^{-7} for a two-qubit gate error).

Long-distance distribution of EPR pairs can severely reduce the fidelity of the EPR pairs arriving at a functional unit for data teleportation, as shown in Figure 9. In order to process 1024 qubits, we could imagine arranging them on a square 32x32 grid, in which the longest possible Manhattan distance is 64 logical qubit lengths. If we assume that we have teleporter units at every logical qubit, EPR pair distribution could require up to 64 teleports. From the figure, teleporting 64 times could increase EPR pair qubit error by a factor of 100. The dotted line represents the threshold at which the EPR pairs must be in order to not corrupt the data qubit when teleporting it. In order to preserve data fidelity, we must use EPR pair purification. One way to think about this process is to stitch Figures 8 and 9 side-by-side, so that EPR pairs accumulate error (degrade in fidelity) as they are teleported and then purified back to a higher fidelity at the endpoints before being used with data.

Latency Difference: Equation 2 shows a linear dependence on distance for ballistic movement latency. Equation 5 also shows that teleportation has a linear dependency on distance as well, but the constant in this case is for the necessary classical communication. We assume classical information can be transferred on a time scale orders of magnitude faster than the quantum operations.

If teleportation is considered performed in near constant time, then we would like to know the distance crossover point where teleportation becomes faster than the equivalent ballistic transport. From Table 1, teleportation takes about $122\mu s$ while ballistic movement takes $0.2\mu s$ per ion trap cell. Thus for a distance of about 600 cells, teleportation is faster than ballistic movement. We assume our communications fabric to be a 2-D mesh of teleporter nodes and use 600 cells as the distance that each teleportation “hop” travels. Allowing teleportations of longer distances would further reduce communication latency in some cases but would then require more local ballistic movement to get an EPR pair from the nearest teleporter to its final destination.

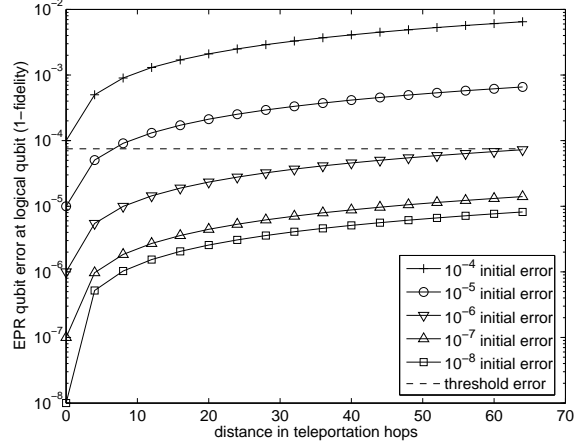


Figure 9: Final EPR error (1-fidelity) as a function of number of teleportations performed, for various initial EPR fidelities. The horizontal line represents the minimum fidelity the EPR pair must be at to be suitable for teleportation of data qubits, $1 - 7.5 * 10^{-5}$

4.7. Purification Resources

Earlier in this section, we noted that when we purify a set of EPR pairs, we measure and discard at least half of them for every iteration. This means that to perform x rounds, we need more than 2^x EPR pairs to produce a single good pair.

To measure EPR resource usage, we count the total number of pairs used *over time* to move a level 2 [27] error corrected logical data qubit between endpoints. This means we are transporting 49 physical data qubits some distance by way of teleportation. We find that the total number of EPR qubits necessary to move a datum critically affects the data bandwidth that our network can support. This metric differs from that used in a number of proposals for quantum repeaters which focus on the layout of a quantum teleporter and are most concerned with spatial EPR resources, i.e. how much buffering is necessary for a particular teleporter in the network [4]. We will show that our design is fully pipelined, and therefore only a small number of qubits must be stored at any place in the network at any time.

We saw in Figure 8 that if we start at a relatively low fidelity and try to obtain a relatively high fidelity, we could need more than a million EPR pairs to produce a single high fidelity pair using the BBPSSW protocol. Therefore we use the DEJMPS protocol in all further analysis. Even though the DEJMPS protocol converges to good fidelity values much quicker, the exponential increase in resources for each additional round performed means we must be careful about how much error we accumulate when distributing EPR pairs. We will also show that the point in the datapath at which purification is performed can have a dramatic impact on total EPR pairs consumed. We have 3 options:

Endpoints only: Purify only at the endpoints, immediately before using EPR pairs to teleport data.

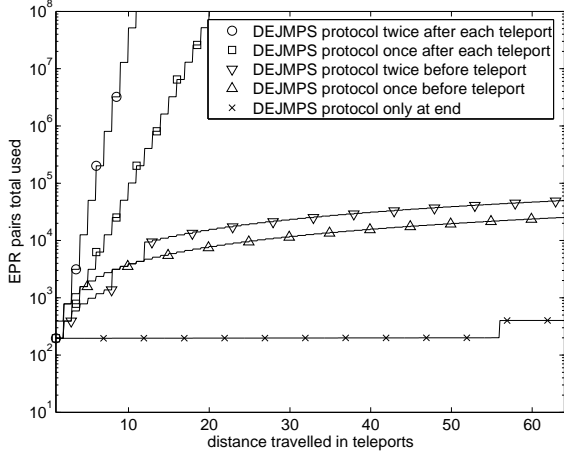


Figure 10: Total EPR pairs consumed as a function of distance and point at which purification scheme DEJMPS is performed.

Virtual wire: Purify EPR pairs which create the links between teleporters, namely the constant stream of pairs from a G node to adjacent T' nodes. The result is higher fidelity qubits used for chained teleportation.

Between teleports: Purify EPR pairs *after* every teleportation; this purifies qubits that are being chain teleported rather than qubits assisting the chained teleportation.

We now model the error present in our entire communication path. Assuming the EPR pairs at the logical qubit endpoints must be of fidelity above threshold, we determine the number of EPR pairs needed to move through different parts of the network per logical qubit communication.

Total EPR Resources: Figure 10 shows that the Endpoints Only scheme uses the fewest total EPR resources. This conclusion is evident if we refer back to Figure 8, where purification efficiency asymptotes at high fidelity; thus, purifying EPR pairs of lower fidelity shows a larger percentage gain in fidelity than purifying EPR pairs of high fidelity. From this, we can see that to minimize total EPR pairs used in the whole system, it makes sense to correct all the fidelity degradation in one shot, just before use.

Non-local EPR Pairs: Another metric of interest is to focus only on those EPR pairs that are transmitted to endpoints during channel setup (i.e. those that are teleported through the path). This resource usage is critical for several reasons: First, every EPR pair moved through the network consumes the slow and potentially scarce resource of teleporters; in contrast, the EPR pairs consumed in the process of producing virtual wires are purely local and thus less costly. Second, because of contention in the network, EPR pairs communicated over longer distances (multiple hops) place a greater strain on the network than those that are

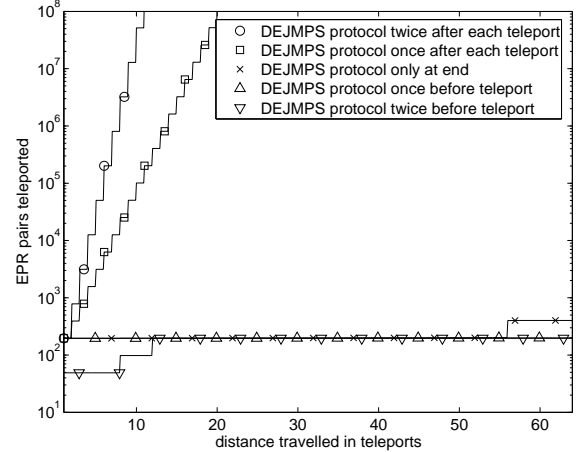


Figure 11: Total EPR pairs in teleportation channel as a function of distance and point in transport in which purification scheme DEJMPS is performed. The only 2 lines that change from Figure 10 are the purify before teleport cases.

transmitted only one hop. The channel setup process can be considered to consume bandwidth on every virtual wire that it traverses. Third, the total EPR pairs transmitted to endpoints during channel setup consumes purification resources at the endpoints—a potentially slow, serial process.

Figure 11 shows that purifying EPR pairs after each teleport transmits many more EPR pairs than purifying at the endpoints (either with or without purifying the virtual wires). From this figure, we see that over-purifying bits leads to additional exponential resource requirements without providing improved final EPR fidelity⁴. Virtual wire purification improves the underlying channel fidelity for everything moving through the teleporters, thereby allowing less error to be introduced into qubits traveling through the channel. For a given target fidelity at the endpoints, virtual wire purification reduces the number of EPR pairs that need to move through the teleporters and also reduces the strain on the endpoint purifiers.

To summarize, we have made the following design decisions based on fidelity and latency concerns:

Teleport data always: Data qubits sent to destination with single teleportation to minimize ballistic error.

Teleport EPR pairs: EPR pairs distributed to endpoints with teleportation, allowing pre-purification to increase the overall fidelity of the network.

Purification before teleport and at endpoints: Purify intermediate EPR pairs before they are used for teleportation as well as EPR pairs at the channel endpoints.

⁴The authors of [4] claim that this nested purification technique (after every teleport) has small resource requirements; however, they count spacial resources rather than total resources over time.

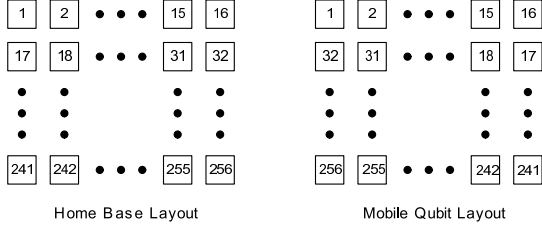


Figure 15: Two possible logical qubit layouts. The Mobile Qubit Layout capitalizes on the sequential nature of QFT.

plementation. First, a tree structure of depth n is implemented with n purifiers (rather than $2^n - 1$, as above). Second, movement between levels of purification is minimized, lessening the impact of movement (which is over an order of magnitude worse than two-qubit gate error; see Table 1). Third, no special handling for lost subtrees due to failed purifications is necessary as they'll be rebuilt naturally.

The primary drawback of this implementation is the latency penalty. If x purifications are needed at level L_0 , then they must necessarily be done sequentially. This problem may be alleviated by including more queues, however, since each logical communication requires multiple high-fidelity EPR pairs, depending upon the encoding used. For these reasons, we use Queue Purifiers in our simulations.

5.2. Benchmarks

We studied Shor's Factorization Algorithm [25], which consists of three communication-intensive components: Quantum Fourier Transform (QFT) on one set of logical qubits, Modular Exponentiation (ME) on another set, and a Modular Multiplication (MM) between the two sets.

QFT contains all-to-all communication between the logical qubits. MM has a bipartite communication pattern, with all from one set communicating with all from the other set. ME consists of squaring steps which require all-to-all communication and multiplication steps which involve bipartite communication. This provides us with two benchmark communication patterns. Since QFT is also a component of many other quantum algorithms [10, 12, 13, 15, 20], we decided to concentrate study on the all-to-all pattern.

A circuit for performing QFT is described in [21]. Given n logical qubits, labeled 1, 2, ..., n , each logical qubit must interact once with each other logical qubit, in numerical order. Thus, the first few communications in QFT are 1-2, 1-3, (1-4, 2-3), (1-5, 2-4), (1-6, 2-5, 3-4), where communications in parentheses may occur simultaneously.

When simulating the Home Base implementation described earlier, we utilize the basic layout shown on the left of Figure 15. Since QFT is a common kernel, it's worthwhile to optimize a bit. So in the case of Mobile Logical Qubits, we simulate the Mobile Qubit Layout in Figure 15. In this layout, logical qubit 1 successively teleports

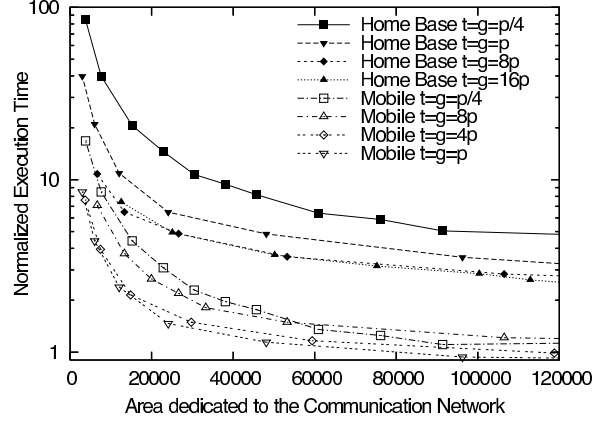


Figure 16: Benchmark execution normalized to execution on $t = g = p = 1024$, as a function of resource allocation.

from logical qubit to logical qubit, being error corrected in place after each logical operation. Once logical qubit 1 has passed, logical qubit 2 can start moving along the line, and so on. Once a logical qubit has completed its interaction with logical qubit 256, it is teleported back to its starting location. Thus, this particular circuit consists primarily of local communications, with the exception of teleports from the final logical qubit location.

5.3. Results

We studied the effects of resource allocation on execution time. Since generation and teleportation have nearly equivalent latency, we match their bandwidth by setting the number of generators g per G node to equal the number of teleporters t per T' node. To avoid deadlock, storage for incoming teleports is not multiplexed, yielding t storage cells per incoming link (yielding $4t$ storage cells per T' node). Given results in Section 4, we will need a maximum purification tree of depth three (for distances under consideration); consequently, we use Queue Purifiers of depth three.

Figure 16 shows the execution time of the benchmarks. Since the expected number of EPR pairs required for the longest communication path is 392 (= pairs for endpoint purification \times qubits per logical qubit = $2^3 \times 49$), we normalized execution time to the execution time for $t = p = g = 1024$ as a close approximation of unlimited resources.

By fixing the area dedicated to the interconnection network (T', G, and P nodes) and varying the size of T' and G nodes relative to P nodes, we can demonstrate where the bottlenecks in the system arise. The Home Base benchmark contains many simultaneously active channels sharing the T' nodes. As more channels share T' nodes, the time multiplexing limits the overall bandwidth of each channel, minimizing the number of purifiers necessary at the end points. As shown in the graph, the limited bandwidth of the channels allows us to allocate more resources to the T' nodes by

sacrificing the number of Queue Purifiers.

In contrast, the Mobile Qubit benchmark contains fewer channels sharing T' nodes, placing a higher demand on the number of Queue Purifiers available at the end point. As we dedicate more and more of the available resources away from P nodes to T' nodes, the performance suffers, as shown in the difference between $t = g = 4p$ and $t = g = 8p$.

6. Conclusion

In this paper, we explored designs for interconnection networks of quantum computers. We accounted for both the flow of quantum bits and the classical information that accompanies it. We simulated a mesh grid architecture under the communication patterns of a common component of many quantum algorithms, the Quantum Fourier Transform, to determine the effects resource allocation will have on performance. We show that devoting sufficient resources to the network is important for performance.

Our study revealed how qubit fidelity is dependent on the errors in quantum operations and the distance of communication. Fidelity degradation is also strongly dependent on the choice of the purification algorithm. Even under the most optimal circumstances, the number of EPR pairs distributed to set up a communication channel is several dozen. This implies the need for an EPR pair distribution infrastructure in a quantum datapath. Not only does this impose the allocation of space for active components (such as teleporters and generators), but it also necessitates temporary storage for qubits as well as an efficient recycling mechanism to allow the constant reuse of qubits.

Finally, we highlighted the need for a classical network to organize this infrastructure. The network must have adequate bandwidth for one in-flight message for each physical qubit in the system as well as the classical bits for each teleportation and purification operation.

References

- [1] V. S. Adve and M. K. Vernon. Performance analysis of mesh interconnection networks with deterministic routing. *IEEE Trans. on Parallel and Dist. Systems*, 5(3):225–246, 1994.
- [2] C. H. Bennett, G. Brassard, S. Popescu, B. Schumacher, J. A. Smolin, and W. K. Wootters. Purification of noisy entanglement and faithful teleportation via noisy channels. *Phys. Rev. Lett.*, 76:722, 1996.
- [3] C. H. Bennett and et. al. Teleporting an Unknown Quantum State via Dual Classical and EPR Channels. *Phys. Rev. Lett.*, 70:1895–1899, 1993.
- [4] L. Childress and et. al. Fault-tolerant quantum repeaters with minimal physical resources, and implementations based on single photon emitters. *quant-ph/0502112*, 2005.
- [5] W. J. Dally. Performance Analysis of k-Ary n-Cube Interconnection Networks. *IEEE Trans. on Computers*, 39(6):775–785, 1990.
- [6] D. Deutsch, A. Ekert, and et. al. Quantum Privacy Amplification and the Security of Quantum Cryptography Over Noisy Channels. *Phys. Rev. Lett.*, 77:2818, 1996.
- [7] W. Dur, H. J. Briegel, and et. al. Quantum repeaters based on entanglement purification. *Phys. Rev.*, A59:169, 1999.
- [8] P. Hazucha and C. Svensson. Impact of CMOS technology scaling on the atmospheric neutron soft error rate. *IEEE Trans. on Nuclear Science*, 47:2586–2594, 2000.
- [9] W. K. Hensinger and et. al. T-junction ion trap array for two-dimensional ion shuttling, storage and manipulation. *quant-ph/0508097*, 2005.
- [10] L. Ip. Solving Shift Problems and Hidden Coset Problem Using the Fourier Transform. *quant-ph/0205034*, 2002.
- [11] N. Isailovic and et. al. Datapath and Control for Quantum Wires. *Trans. on Arch. and Code Optimization (TACO)*, 1:34–61, 2004.
- [12] R. Jozsa. Quantum Algorithms and the Fourier Transform. *Proc. Roy. Soc. London Ser A*, 454:323–337, 1998.
- [13] R. Jozsa. Quantum Factoring, Discrete Logarithms and the Hidden Subgroup Problem. *quant-ph/0012084*, 2000.
- [14] D. Kielpinski, C. Monroe, and D. Wineland. Architecture for a large-scale ion-trap quantum computer. *Nature*, 417:709–711, 2002.
- [15] A. Kitaev. Quantum measurements and the Abelian Stabilizer Problem. *quant-ph/9511026*, 1995.
- [16] E. Knill and R. Laflamme. Theory of quantum error-correcting codes. *Phys. Rev. A*, 55:900–911, 1997.
- [17] D. Leibfried and et al. Experimental demonstration of a robust, high-fidelity geometric two ion-qubit phase gate. *Nature*, 422:412–415, 2003.
- [18] M. Madsen, W. Hensinger, D. Stick, J. Rabchuk, and C. Monroe. Planar ion trap geometry for microfabrication. *Applied Physics B: Lasers and Optics*, 78:639 – 651, 2004.
- [19] T. S. Metodi, D. D. Thaker, A. W. Cross, F. T. Chong, and I. L. Chuang. A Quantum Logic Array Microarchitecture: Scalable Quantum Data Movement and Computation. In *Proc. of Intl. Symp. on Microarchitecture (MICRO)*, 2005.
- [20] M. Mosca and A. Ekert. The Hidden Subgroup Problem and Eigenvalue Estimation on a Quantum Computer. *Proc. of the 1st NASA Intl. Conf. on Quantum Comp. and Quantum Comm.*, 1999.
- [21] M. A. Nielsen and I. L. Chuang. *Quantum Computation and Quantum Information*. Cambridge University Press, Cambridge, UK, 2000.
- [22] M. Oskin, F. T. Chong, I. L. Chuang, and J. Kubiatowicz. Building Quantum Wires: The Long and the Short of it. In *Proc. of Intl. Symp. on Comp. Arch. (ISCA)*, 2003.
- [23] R. Ozeri and et. al. Hyperfine Coherence in the Presence of Spontaneous Photon Scattering. *E-Arxiv: quant-ph/0502063*, 2004.
- [24] M. A. Rowe and et. al. Transport of quantum states and separation of ions in a dual RF ion trap. *Quant. Inf. Comp.*, 2:257–271, 2002.
- [25] P. Shor. Polynomial-Time Algorithms For Prime Factorization and Discrete Logarithms on a Quantum Computer. *35th Ann. Symp. on Foundations of Comp. Science (FOCS)*, pages 124–134, 1994.
- [26] P. W. Shor. Scheme for reducing decoherence in quantum computer memory. *Phys. Rev. A*, 54:2493, 1995.

- [27] A. Steane. Error correcting codes in quantum theory. *Phys. Rev. Lett*, 77:793–797, 1996.
- [28] K. Svore and et. al. Local Fault-Tolerant Quantum Computation. *Phys. Rev. A*, 72:022317, 2005.
- [29] D. Wineland and T. Heinrichs. Ion Trap Approaches to Quantum Information Processing and Quantum Computing. *A Quantum Information Science and Technology Roadmap*, page URL: <http://quist.lanl.gov>, 2004.
- [30] W. Wootters and W. Zurek. A Single Quantum Cannot Be Cloned. *Nature*, 299:802–803, 1982.